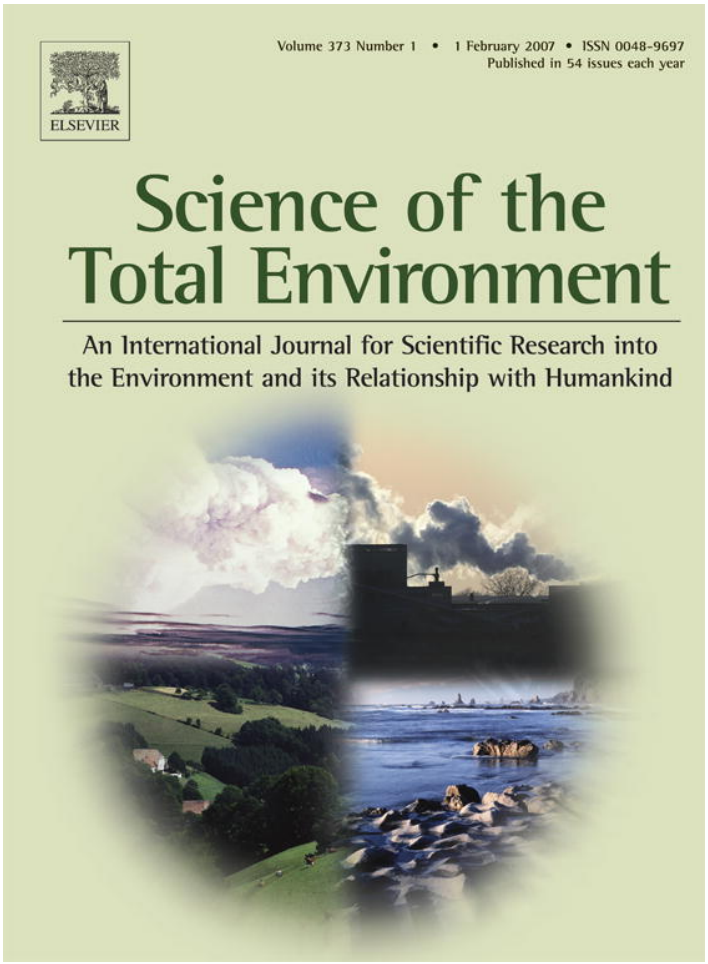

Available online at www.sciencedirect.com
ScienceDirect
Science of the Total Environment 373 (2007) 305–323
Science of the Total Environment
An International Journal for Scientific Research into the Environment and its Relationship with Humankind
www.elsevier.com/locate/scitotenv

Discriminatory classification of natural and anthropogenic waters in two U.K. estuaries

Robert G.M. Spencer [a,*], Andy Baker [b], Jason M.E. Ahad [c,1], Gregory L. Cowie [c], Raja Ganeshram [c], Robert C. Upstill-Goddard [a], Günther Uher [a]

[a] *Ocean Research Group, School of Marine Science and Technology, The Ridley Building, University of Newcastle-upon-Tyne, NE1 7RU, UK*
[b] *School of Geography, Earth and Environmental Sciences, University of Birmingham, Edgbaston, Birmingham, B15 8TT, UK*
[c] *School of GeoSciences, Kings Buildings, University of Edinburgh, EH9 3JW, UK*

Received 19 May 2006; received in revised form 20 October 2006; accepted 26 October 2006
Available online 22 December 2006

Abstract

The ability to distinguish water inputs from both natural and anthropogenic sources was investigated in the complex environment of an urban estuary (Tyne) and a relatively pristine estuary (Tweed). We used a data set from a total of 11 estuarine transects, comprising measurements of bulk dissolved organic matter (dissolved organic carbon and nitrogen), dissolved nitrogen (total dissolved nitrogen, ammonium, nitrate+nitrite and dissolved organic nitrogen), optical absorbance measurements (a_{350}, $S_{290-350}$) and fluorescence excitation emission matrix measurements (fluorophores A, H, B and T intensity and A and H emission wavelength maxima). In order to investigate trends within the numerous parameters measured, multivariate statistics were employed. Principal components analyses showed 63.4% of the variability in the total data set can be explained by two sets of components and 74.9% of the variability by the spectrophotometric measurements alone. In both analyses the first component correlated to the mixing of terrestrial and marine waters and the second component was correlated to sources of pollution such as domestic sewage. Within the data set, river flow and terrestrially derived DOM were significantly correlated, and situations with high river input showed an increase in terrestrial signature in the estuary. Discriminant analyses were also carried out and indicated that 59.8% (total data set) and 53.3% (solely spectrophotometric data) of the samples can be correctly classified into their respective groups (water categories) assigned on the basis of salinity and sampling location. Overall the results clearly show the potential of spectrophotometric techniques to discriminate distinct water categories with different DOM characteristics. In particular, measurement of the fluorophore H emission maxima, the spectral slope parameter, $S_{290-350}$, and fluorophores T and B intensity enabled discrimination of DOM from riverine, estuarine, marine, and sewage affected water categories. The results presented here indicate the ability of spectrophotometric data alone to distinguish between marine, anthropogenic and terrestrial DOM and distinguish terrestrial DOM from different catchments (Tyne vs. Tweed). With current advances in the in-situ deployment of absorbance and fluorescence spectroscopy it is anticipated that multivariate statistics will gain importance as a cost effective, powerful and diagnostic approach to assessing the distributions of water types and their associated DOM characteristics and fluxes at the land–ocean interface.

Keywords: Dissolved organic matter; Absorbance; Fluorescence; Tyne; Tweed; Estuarine

* Corresponding author. Now at: Department of Land, Air and Water Resources/Department of Viticulture and Enology, University of California, Davis, One Shields Avenue, CA 95616, USA. Tel.: +1 530 754 4327; fax: +1 530 752 0382.
E-mail address: rgspencer@ucdavis.edu (R.G.M. Spencer).
[1] Now at: Environmental Engineering Research Centre, School of Planning, Architecture and Civil Engineering, David Keir Building, Queen's University Belfast, BT7 1NN, U.K.

0048-9697/$ - see front matter © 2006 Elsevier B.V. All rights reserved.
doi:10.1016/j.scitotenv.2006.10.052

1. Introduction

The role of dissolved organic matter (DOM) in global carbon cycling in general, and in the photoproduction of climatically active trace gases and other biogeochemically reactive species, is receiving increased interest within the context of global change. DOM also plays central roles in the fate, reactivity and transport of inorganic and organic pollutants. The riverine fluxes of DOM and inorganic nutrients have important impacts on the marine system (Dittmar and Kattner, 2003), yet the fate of terrigenous DOM and inorganic nutrients in marine environments, and their estuarine dynamics are poorly understood (Hedges et al., 1997; Hedges and Keil, 1999). Although estuaries account for only ~0.4% of the marine system by area they have been shown to be regions of intense biogeochemical activity with great potential for modifying the riverine supply of reactive species to the oceans (Morris et al., 1978). Estuaries are highly complex environments and have been described as one of the most difficult environments on Earth in which to investigate the origins, pathways and fates of dissolved materials (Hedges and Keil, 1999). In addition to the complex physical and biogeochemical processes estuaries often suffer from intense anthropogenic perturbation (e.g. cities, ports, heavy industry) further compounding the problems of understanding and delineating the processes which occur in this environment. Therefore estuaries represent one of the most challenging yet most relevant environments for which discrimination of DOM source is important.

DOM absorbs light in the visible, UV-A and UV-B wavelength ranges. Previous work has often used the light absorbance of the chromophoric fraction of DOM (CDOM) to predict dissolved organic carbon (DOC) concentrations from in-situ optical measurements and optical remote sensing (Ferrari et al., 1996; Vodacek et al., 1995). Further work has led to the use of spectral absorbance properties to distinguish compositional characteristics, and discriminate between terrestrial and marine DOM in particular (e.g. Blough and Del Vecchio, 2002). Numerous studies, for example, have utilised CDOM as a tracer of terrigenous inputs to the coastal ocean (Blough et al., 1993; Vodacek et al., 1997; Del Castillo et al., 1999). CDOM light absorption is highest in the UV region; it declines approximately exponentially with increasing wavelength and is generally broad and unstructured (Bricaud et al., 1981; Blough and Green, 1995). Spectral CDOM absorbance is often described by a single exponential model

$$a_\lambda = a_{\lambda o} e^{-S(\lambda-\lambda o)} \quad (1)$$

where a_λ and $a_{\lambda o}$ are CDOM absorption coefficients (m^{-1}) at wavelength λ and reference wavelength λo (nm) and S is the spectral slope (nm^{-1}). S defines the spectral dependence of the CDOM absorption coefficient and as a result provides information in relation to the nature of the CDOM (Blough and Del Vecchio, 2002). S has been shown to vary with the source of CDOM and also to change in response to biological and chemical alteration of the source material (Blough and Del Vecchio, 2002). For example, S, is typically steeper for marine waters than freshwaters and it typically increases with decreasing absorption coefficients and increasing salinity in estuaries (Blough et al., 1993; Green and Blough, 1994; Blough and Del Vecchio, 2002). The relatively shallow values of S in freshwaters are thought to be characteristic of their terrigenous origin and relative lack of photochemical and biological alteration, whereas the steeper values of S in marine waters have been attributed either to their autochthonous source or to photochemical degradation in the marine photic zone (Blough and Del Vecchio, 2002). S has also been related to a number of molecular properties and has been shown to become steeper with decreasing molecular weight and decreasing aromaticity (Blough and Green, 1995; Stubbins, 2001). Thus, the shallow S of riverine DOM may indicate that terrestrial material is richer in high molecular weight DOM and has a higher aromatic content compared to marine DOM.

Following the work by Coble et al. (1990) three-dimensional excitation, emission matrix (EEM) spectra have been used for investigating the fluorescence properties of CDOM. EEM spectra are acquired by sequential fluorescence emission scans at successively increasing excitation wavelengths, and consist of three-dimensional spectra showing excitation and emission wavelengths and fluorescence intensity. An EEM typically covers a range of excitation and emission wavelengths from ~200 nm (short wavelength UV) through to ~500 nm (visible blue-green light), and may contain fluorescence centres that are attributable to both natural DOM groups such as humic and fulvic-like material, as well as fluorescent protein-like material (Coble et al., 1990; Coble, 1996; Baker, 2001, 2002a). Coble (1996) named the humic and fulvic-like material fluorescence centres as fluorophores A, C and M; fluorophores C and M are often described together as fluorophore H (Del Castillo et al., 1999). Marine samples typically show fluorophore H at excitation and emission wavelengths shorter than those observed for related humic-like fluorophores in terrestrial DOM, most commonly with a blue-shift for excitation and emission by ~25 nm and ~5–30 nm, respectively (Coble, 1996; Del Castillo et al., 1999). Such

a hypsochromic shift in fluorophore H emission has been attributed to the photochemical or microbial breakdown of terrigenous DOM, its mixing with or replacement by a less aromatic marine DOM, or a combination thereof (Coble, 1996; Blough and Del Vecchio, 2002). Protein-like fluorophores T and B (Coble, 1996) have been observed in both marine and freshwaters (Mopper and Schultz, 1993; Coble, 1996; Wu and Tanoue, 2001; Alberts et al., 2004) and were found to occur at enhanced levels in waters impacted by domestic sewage and other wastes (Baker, 2002a,b; Baker et al., 2003). Fluorophores A and H typically have elongated contours, as opposed to rounded contours likely due to multiple fluorescent components or inter-molecular energy transfer (Coble et al., 1990). The measurement of a fluorophore at an excitation–emission wavelength pair is thus unlikely due to a single component and recent studies applying multivariate data analysis techniques such as PARAFAC are increasing our understanding of the complex nature of three-dimensional EEMs (Stedmon et al., 2003; Stedmon and Markager, 2005; Holbrook et al., 2006).

A variety of optical, spectroscopic techniques are now being used comprehensively to characterise CDOM in natural waters. Recent technological advances led to the development of in-situ techniques for the real-time analyses of natural waters at selected excitation wavelengths with high spatial and temporal resolution (Hart and Jiji, 2002; Chen and Gardner, 2004; Baker and Inverarity, 2004). Furthermore, advances in commercially available bench top spectrofluorometers now allow rapid generation of EEMs extending into the shortwave UV (>200 nm), and thus facilitate the identification of fluorescence centres with shortwave excitation and emission maxima. The aim of this study was to investigate the potential of multivariate statistics to categorise and distinguish different surface waters on the basis of bulk DOM (dissolved organic carbon and nitrogen), dissolved nitrogen content (total dissolved nitrogen, ammonium, nitrate+nitrite and dissolved organic nitrogen), optical absorption measurements (a_{350}, $S_{290-350}$) and fluorescence EEM measurements (Fluorophores A, H, B and T intensity and A and H emission wavelength maxima). Our study focused on a data set comprising 11 estuarine transects from the Tyne and Tweed estuaries located on the North Sea coast of northeast England. Statistical data analysis (SPSS Version 11) was employed to investigate trends in the data set and to examine which of the parameters measured was potentially the most useful for discriminating between different water categories within each estuary and also between different estuaries (Tyne and Tweed).

2. Materials and methods

2.1. Study sites

The River Tyne (Fig. 1a) has a catchment area of 2935 km^2 and a mean freshwater discharge of ~45 m^3 s^{-1}. There are two main tributaries, the North Tyne, which has its source in the Cheviot Hills (mean altitude ~500 m) near the Scottish Border, and the South Tyne which rises in the Cumbrian Pennines (mean altitude ~800 m). Soils in the catchment are dominated by large areas of peat in the uplands, which provides a substantial store of organic carbon, and with stagno-gleys in the majority of the remaining areas. In general the soils are slow draining, and are underlain by shallow or low permeability aquifers, leading to the hydrology of many sub-catchments being dominated by surface runoff with rapid response to rainfall as a result of saturation excess. The North and South Tyne combined provide ~90% of the freshwater discharge into the estuary. The two rivers join to form the River Tyne, which flows in an easterly direction to Wylam, where it becomes tidal for the last ~33 km of its course. Other tributaries of the Tyne estuary are the polluted urban rivers Derwent, Team and Ouseburn which account for the remaining ~10% of the total freshwater discharge into the estuary. Upstream of Wylam, the catchment is predominantly rural, whereas below Wylam an urban population of approximately 900,000 influences the water quality of the estuary, with 214 consented discharges from sewage treatment works, 126 consented industrial discharges and 492 storm sewage discharges. Areas of poor water quality are predominantly centered on the urbanised areas around the city of Newcastle-upon-Tyne (including the lower reaches of the rivers Derwent and the Ouseburn) with many sewage inputs and without substantial upland clean water supplies to dilute them. The Tyne Estuary (Fig. 1a) is a partially mixed mesotidal estuary which experiences significant stratification during neap tides, although the estuary can be well mixed during spring tide episodes. Mean freshwater residence times range from ~6.3 to 23.4 days with an annual mean of ~11.7 days. Industrial fluxes to the lower estuary are declining. However the Tyne estuary continues to receive significant urban waste in the form of secondary treated sewage from Howdon sewage treatment works (STW). This STW can be an important contributor of dissolved nutrients and organic matter to the lower estuary and is the third largest estuarial discharge in the U.K., dealing with waste from ~900,000 people.

The River Tweed and its tributaries drain a rural, relatively sparsely populated region of the Anglo-

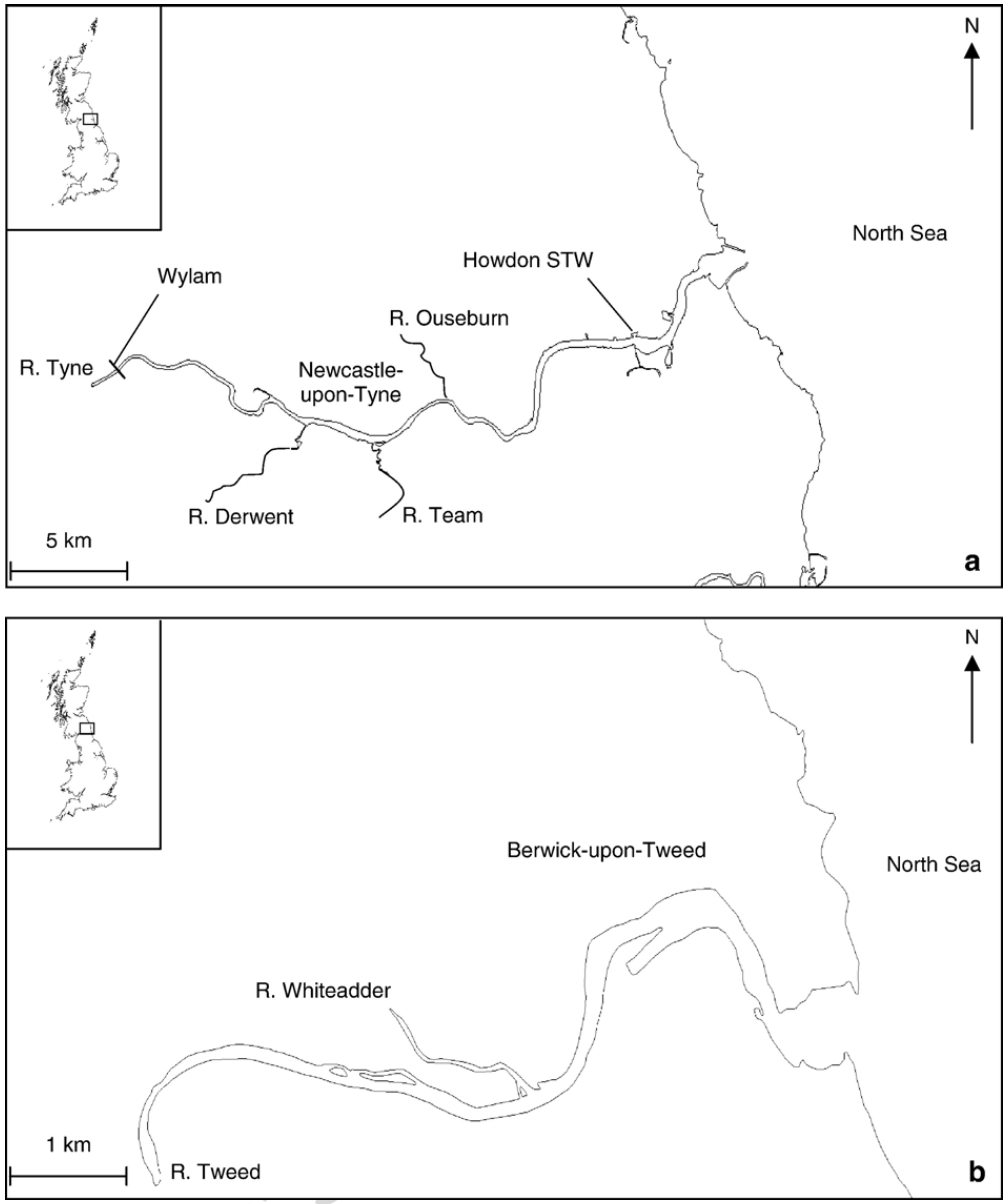

Fig. 1. (a) Map of the Tyne estuary. (b) Map of the Tweed estuary.

Scottish borders. Most of the Tweed's discharge originates from the main river, although approximately 10% of the freshwater input comes from the Whiteadder (Fig. 1b), which joins the Tweed approximately 6.5 km inland from the North Sea. The combined catchment area of the Tweed and Whiteadder is approximately 4900 km^2 and the average freshwater input into the estuary is ~84 $m^3 s^{-1}$ (Fox and Johnson, 1997). The maximum length of the Tweed estuary (Fig. 1b) is around 13 km and the residence time is approximately 1 day (Uncles and Stephens, 1996). The Tweed is a partially mixed to stratified microtidal estuary (Uncles and Stephens, 1996). The catchment is dominated by agricultural activity, ranging from upland areas of peat moorland used for sheep grazing to more arable regions in the lowlands. The Tweed receives significantly less anthropogenic inputs than the Tyne and in general the water quality in the Tweed drainage basin is good (Robson and Neal, 1997).

2.2. Estuarine sampling

Estuarine samples were collected on 11 single day axial transects at sites based on in-situ salinity measurements using a portable probe (Horiba model U-10; or Hanna Instruments, model HI 8633) in order to allow high-resolution coverage of the full estuarine salinity gradient. Sampling in both Tyne (9 axial transects) and Tweed (2 axial transects) estuaries was predominantly at high tide to permit boat access to the inner-estuary.

However, on two occasions (04-10-2002 and 23-07-2003) due to the risk of grounding the boat in the Tyne estuary no low salinity samples could be taken. Conversely on one Tyne transect (01-08-2002) a full salinity North Sea sample was not collected due to the freshwater plume extending considerably offshore and weather conditions not permitting safe offshore sampling to be conducted on that day.

Estuarine water samples were collected from 1 m depth and filtered immediately through 0.7 μm (Whatman GF/F) precombusted (450 °C) filters and the filtrate was collected directly in an acid cleaned, precombusted (550 °C) glass vial with a Teflon-lined cap. Samples were then stored at 4 °C in the dark until return to the laboratory. Samples for DOC/TDN analyses were then acidified to pH ~2 and refrigerated (4 °C) if the samples were to be analysed within 2 weeks, or frozen (−20 °C) for storage of greater than 2 weeks. Samples for both CDOM measurements and dissolved inorganic nitrogen analyses were stored at 4 °C in the dark until analyses (<24 h).

2.3. Analytical methods

2.3.1. Measurement of CDOM absorbance properties

CDOM spectrophotometric analysis used a double beam UV–visible spectrophotometer (Kontron Instruments, Uvicon 923). Instrument precision quoted by the manufacturer is 0.001 absorbance units (AU), corresponding to absorption coefficients of 0.043 m^{-1} and 0.004 m^{-1} for 10 mm and 100 mm pathlength cuvettes, respectively. All samples were measured in duplicate within 24 h of collection using quartz cuvettes, which had been rinsed with hydrochloric acid (0.1 M) and copious amounts of analytical grade water (Milli-Q) from a laboratory system (Millipore Milli-Q plus 185), and then triple rinsed with sample before use. Short pathlength (10 mm) cuvettes were typically used for riverine and estuarine samples (absorbance ≥0.02 at 350 nm). If samples measured in a 10 mm pathlength cuvette exhibited absorbance values <0.02 at 350 nm they were measured in long pathlength (100 mm) cuvettes (e.g. high salinity/North Sea samples). All sample spectra were referenced to a blank spectrum of Milli-Q water. Spectra were scanned over the wavelength range 250–800 nm and corrected for an occasional small offset, arising from possible long-term baseline drift or the entrainment of glass fibre particles in filtered samples (Blough et al., 1993), by subtracting the average absorbance between 700 and 800 nm. To minimise temperature effects all samples were allowed to reach laboratory temperature prior to measurement. All absorbance data in this paper are expressed as $a(\lambda)$ in units of m^{-1}. CDOM absorption coefficients, $a(\lambda)$, were calculated from:

$$a(\lambda) = 2.303A(\lambda)/l \quad (2)$$

where $A(\lambda)$ is the absorbance and l is the cell pathlength in metres (Green and Blough, 1994). Samples in this study ranged in absorbance at 350 nm from 0.374 to 0.002 (10 mm pathlength) and for measurement of highly absorbing samples (≥0.1) dilution was undertaken until absorbance at 350 nm fell below 0.1 (10 mm pathlength). CDOM absorption coefficients were observed to decrease approximately exponentially with increasing wavelengths, as found previously in natural waters (Bricaud et al., 1981; Blough and Green, 1995; Fig. 2a). The linearised spectra were used to determine the spectral slope, S, over the wavelength range 290–350 nm ($S_{290–350}$) (Fig. 2b). In previous studies S has been measured over a wide range of wavelengths (Blough and Del Vecchio, 2002; Twardowski et al., 2004); hence directly comparing these data is problematic. Furthermore, previous work derived S predominantly from a linear least squares regression of the log-transformed absorption data (Bricaud et al., 1981; Blough et al., 1993; Vodacek et al., 1997; Del Vecchio and Blough, 2004), while some recent work used nonlinear least squares fit procedures that avoid the bias caused by the log-transformation of the absorbance spectra (Stedmon et al., 2000; Kowalczuk et al., 2003; Twardowski et al., 2004). We chose to calculate S over the wavelength range 290–350 nm, because Stubbins (2001) showed this range to be sensitive to photobleaching and changes in CDOM chemical composition such as the degree of aromaticity. In addition, as $S_{290–350}$ is in the short wavelength range it is more accurate, chiefly due to higher absorption coefficients at shorter wavelengths. $S_{290–450}$ ($\times 10^{-3}$) was measured for the purpose of comparison with existing data. In the R. Tyne $S_{290–450}$ ($\times 10^{-3}$) was found to range from 13.9 to 15.8 nm^{-1} (mean 14.9 nm^{-1}, $n=7$) and in the R. Tweed from 15.2 to 16.5 nm^{-1} (mean 15.9 nm^{-1}, $n=2$), which is within the S range of 14–17 nm^{-1} reported for a number of major world rivers (Blough and Del Vecchio, 2002) recorded over the same S range. $S_{290–450}$ ($\times 10^{-3}$) for marine endmembers in the Tyne estuary ranged from 13.7 to 18.6 nm^{-1} (mean 15.6 nm^{-1}, $n=9$) and in the Tweed estuary ranged from 15.3 to 17.7 nm^{-1} (mean 16.5 nm^{-1}, $n=2$). Both are comparable to the S range of 13–18 nm^{-1} for coastal waters subjected to riverine inputs (Blough and Del Vecchio, 2002) measured over the same S range. Comparison of S for riverine and

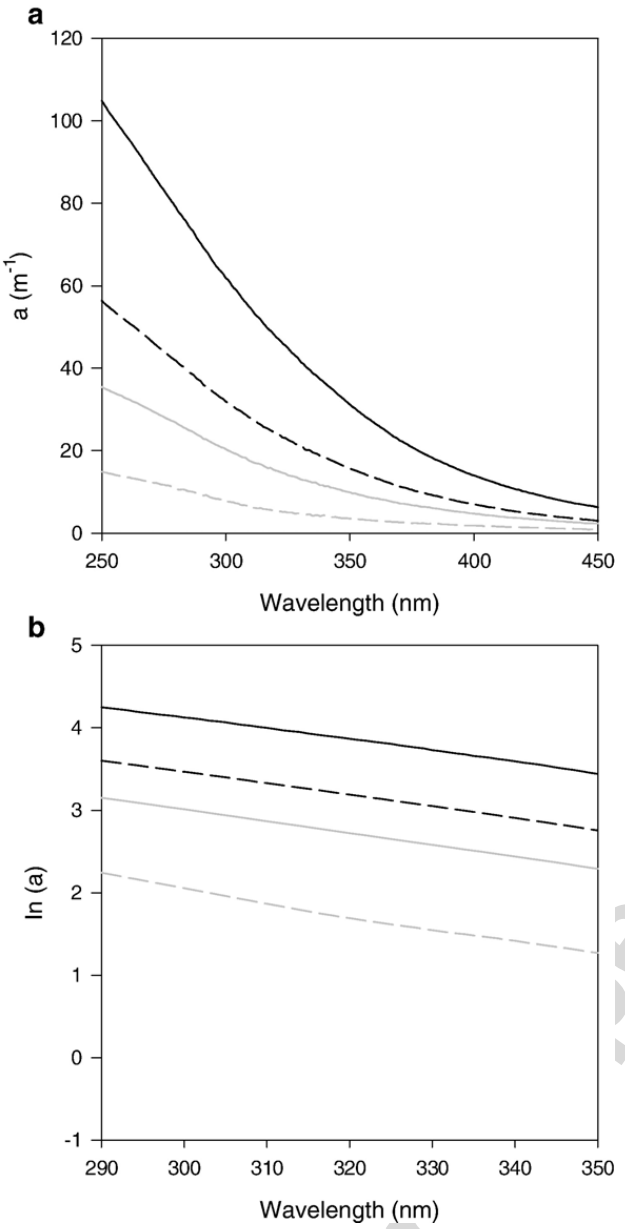

Fig. 2. (a) Typical absorption spectra of water samples collected from the Tyne Estuary (03-03-2003) and their log-linearised form over the spectral slope range used in this study. (b) Solid black line — salinity 0.1; dashed black line — salinity 10.5; solid grey line — salinity 19.0 and dashed grey line — salinity 34.1.

coastal waters determined over the wavelength range 290–450 nm showed a high degree of overlap. Hence, this parameter did not appear to be a highly sensitive measure of changes in CDOM in our case. Our goal within this study was ultimately to discriminate between different water sources and not to compare *S* quantitatively with previous work particularly in light of the problems outlined above in such comparisons. In contrast, *S* determined by linear least squares regression of the log-transformed absorption data over the wavelength range 290–350 nm has been shown to be a useful diagnostic tool in the characterization of CDOM (Stubbins, 2001; Kitidis et al., 2006) and was therefore adopted for this work.

2.3.2. Measurement of CDOM fluorescence properties

DOM fluorescence measurements were made using both a Perkin-Elmer LS-50B and a Varian Cary Eclipse spectrofluorometer. Both spectrofluorometers used a xenon excitation source, and slits were set to 5 nm for both excitation and emission. Validation was performed daily using a sealed water cell containing pure water and the Raman peak intensity of water at 348 nm was used to monitor instrument stability and to permit inter-laboratory comparison. Results were normalised to a mean measured Raman peak intensity of 20.0±0.3 arbitrary units as previously described by Elliot et al. (2006) and Baker (2005). To produce fluorescence excitation–emission matrices (EEMs) (Fig. 3), excitation wavelengths were incremented from 200 to 420 nm at 5 nm intervals; for each excitation wavelength the emission was detected from 280 to 500 nm at 0.5 nm intervals. Analysis was performed and EEMs produced using Perkin-Elmer FL WinLab and Varian Cary Eclipse software. For each water sample, the fluorescence peaks were measured at the maximum fluorescence intensity (FI) at an excitation–emission wavelength pair. This data on normalisation to the Raman peak intensity is referred too in intensity units (I.U.) in this study and where emission maxima (Em.) of fluorophores is discussed this refers to the emission wavelength of the maximum FI. An intercalibration experiment was conducted between the two spectrofluorometers with River Tyne water. On comparison of the FI of the major fluorophores measured on both instruments a strong correlation was found (r^2=0.96, FI (Varian)=FI (Perkin Elmer)+16.7; all data were normalised to the Varian Cary Eclipse). Duplicate scans of the same sample were typically consistent within ≤5% with respect to FI and within ≤2% with respect to fluorophore emission maxima location.

In the literature fluorescence is sometimes also reported in quinine sulphate units (QSU) (Coble et al., 1993; De Souza Sierra et al., 1994; Skoog et al., 1996), although most recent work generally reports FI normalised to the Raman signal of water. To facilitate comparison with results reported in QSU and results reported here in intensity units normalised to the Raman peak, a quinine sulphate dihydrate (Aldrich) solution in 0.05 M sulphuric acid (Skoog et al., 1996) was made. One quinine sulphate unit (QSU) corresponds to the fluorescence of a 1 μg l^{-1} quinine sulphate dihydrate solution in 0.05 M H_2SO_4. Fluorescence in QSU was measured at an excitation of 350 nm and an emission wavelength of

450 nm as described by Skoog et al. (1996). The bandwidth was set to 5 nm. Table 1 presents fluorophore H fluorescence intensities for a subset of samples from the North Sea and River Tyne, expressed both in QSU and intensity units normalised to the Raman peak.

Table 1 shows a range of QSU values for fluorophore H in North Sea water from 4.1 to 5.5, which is comparable to data from the Southern North Sea with a value of 4.7 QSU (Uher and Andreae, 1997). Therefore the FDOM data described here are comparable with previously reported data in QSU. However, all data presented in this paper are reported as intensity units normalised to the Raman peak in order to facilitate comparison with recent work (Stedmon et al., 2003).

Table 1
Fluorophore H quinine sulphate units and intensity units normalised to Raman for North Sea and River Tyne samples

Date	Sample	QSU	Intensity units
13-08-2002	Seawater (33.5)	5.5	15.8
19-03-2003	Seawater (33.5)	4.2	12.6
04-04-2003	Seawater (33.6)	4.1	12.2
13-08-2002	R. Tyne	162.0	403.3
19-03-2003	R. Tyne	59.7	150.1
04-04-2003	R. Tyne	62.7	162.5

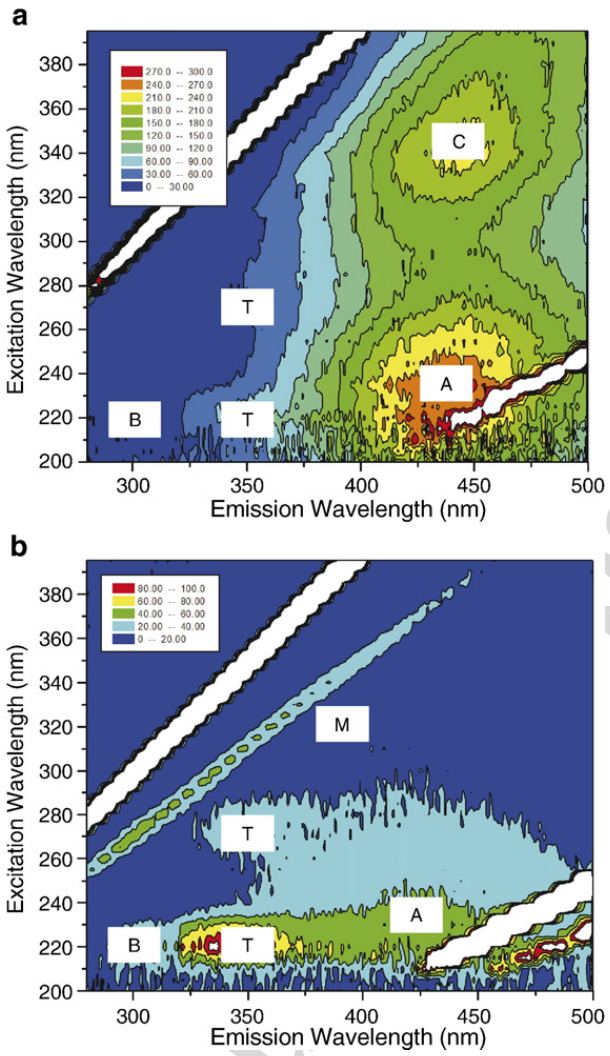

Fig. 3. Typical fluorescence EEMs observed in this study showing the position of the principal fluorophores in optical space: (a) River Tyne, (b) coastal North Sea. C=terrestrial humic/fulvic-like peak; M=marine humic/fulvic-like peak; A=humic-like peak; T=tryptophan-like, protein-like peak; B=tyrosine-like, protein-like peak. Note that the fluorescence intensity scale is different for (a) and (b). Fluorophores C and M are often referred to as H, humic/fulvic-like peak (Del Castillo et al., 1999) for comparison; and where fluorophore T is discussed or used in analyses the lower excitation fluorophore is described as this was always more prominent. The linear features are Rayleigh Tyndall and Raman scattering of water, respectively.

Water samples were analysed in duplicate within 24 h of collection. Analysis was in 10 mm pathlength quartz cuvettes, which were rinsed with hydrochloric acid (0.1 M), copious amounts of Milli-Q water and then triple rinsed with sample before use. To minimise temperature effects all samples were allowed to reach laboratory temperature prior to measurement. All samples measured for fluorescence initially had an absorbance at 350 nm of ≤ 0.1 (10 mm pathlength) due to dilution of samples for measurement of absorbance.

At high DOM concentrations light absorption of the chromophores within the sample itself interfere with excitation and emission resulting in suppressed fluorescence intensity (Bashford and Harris, 1987) called inner-filter effects (IFE). There are a number of methods that can be applied to reduce or remove the effects of absorbance; the simplest of these are dilution to low optical densities or the application of a correction formula. The use of both of these techniques was examined to determine a suitable method of correction for IFE in this study. Another approach, which has also been suggested, is the measurement of fluorescence emission at long excitation wavelengths, for example 370 nm (McKnight et al., 2001) due to the comparatively lower influence of sample absorbance at such wavelengths. However, this method has not been considered as a large amount of information would be lost from the EEM if this technique was employed and additionally even at longer wavelengths IFEs were observed in our CDOM-rich samples (data not shown). Therefore, a comparison was made between diluted and formula corrected samples using the formula:

$$I = I_0(10^{-b(A_{ex}+A_{em})}) \quad (3)$$

where I is the detected fluorescence intensity and I_0 is the fluorescence in the absence of self-absorption. The

factor *b* assumes that both emission and excitation only pass through 0.5× cuvette path length. A_{ex} and A_{em} are the absorbance of the solution at the excitation and emission wavelengths respectively (Ohno, 2002). No significant difference was found between the fluorescence intensities of the diluted samples and the fluorescence intensities of undiluted samples corrected using Eq. (3) (n=20, standard deviation 0.75%). In order to confirm that sample dilution removed any IFEs and that the relationship between absorbance and intensity is linear, a dilution series has to be made for each individual sample. This is both time consuming in terms of preparation and analysis, and it also requires a greater volume of sample. Furthermore, analyses of diluted samples result in observations of DOM that no longer refer to its natural state. For example dilution can cause changes in pH which may alter fluorescence intensity (Westerhoff et al., 2001; Patel-Sorrentino et al., 2002) and lead to spectral shifts (Vodacek, 1992; Mobed et al., 1996). Therefore for the purposes of this study Eq. (3) was used to correct for any IFEs.

2.3.3. Measurement of DOC/TDN

Coupled high temperature catalytic oxidation (HTCO), total organic carbon (TOC) and nitrogen chemiluminescence detection (NCD) was used for the simultaneous measurement of DOC and TDN from the same sample; namely a Shimadzu TOC 5000A coupled to either a Sievers NCD 255 or an Antek 705E. After removal of DIC by acidification and sparging (ca. 8 min at 75 ml min^{-1}) with carbon free gas (Ultra pure oxygen as sparging and carrier gas; BOC 99.999%) 100 µl of sample was injected onto the combustion column. Here the DOC and TDN was oxidised to CO_2, NO and H_2O at 680 °C in the presence of a catalyst (0.5% platinum on aluminium oxide). The combusted gases were subsequently dried using a dehumidifier, purified by means of a halogen scrubber and their CO_2 concentrations determined by a non-dispersive infra-red detector (NDIRD). The signal (voltage) from the NDIRD was recorded using a data collection and integration system and the peak area was used to quantify the DOC concentration. The combustion gases exiting the NDIRD were routed directly into the NCD by means of a vacuum pump. Prior to the gases entering the NCD they were passed through a gas dehumidifier to remove any water vapour not removed by the TOC dehumidifier as moisture quenches the chemiluminescence reaction (Walsh, 1989). The NO in the combustion gases was then reacted with O_3 produced within the NCD to form electronically excited NO_2* which chemiluminesces upon decay to its ground state. The light emitted (hv) was detected by a photomultiplier tube (PMT) and the signal (voltage) was recorded using a data collection and integration system, with peak area used to quantify the TDN concentration. DON concentration was calculated from TDN concentration minus dissolved inorganic nitrogen species concentrations.

As no single compound can represent natural DOM, certified reference materials (CRMs) were used. The CRMs were obtained from the Biogeochemical Group at the Division of Marine and Atmospheric Chemistry, Rosenstiel School of Marine and Atmospheric Science, University of Miami, USA. Deep Sargasso Seawater (44–45 µM C and 21 µM N) was routinely run at the start of every day and between samples and the values obtained in the course of this study (40–48 µM C and 19–22 µM N) are in good agreement with the certified values. An internal standard of Tyne River water (collected 11/07/2002; 733 µM C and 80 µM N) was also run with each batch of DOC and TDN analyses and the values obtained during this study (731.6–735.9 µM C and 77.5–82.2 µM N) are in good agreement with the initial analyses showing consistency of results. The mean of three to five injections of 100 µl is reported for every sample measurement and precision, described as a coefficient of variance (C.V.), was <2% for the replicate injections.

2.3.4. Measurement of dissolved inorganic nitrogen species

Nutrient analyses were carried out following established protocols with a Skalar San^{plus} analyser. The instrument employs air-segmented flow analysis (SFA), with spectrophotometric colour detection. The nutrient under investigation reacts to form a coloured compound and the absorbance of the colour is then determined spectrophotometrically. NO_3^- plus NO_2^- was determined by a method whereby NO_3^- is first reduced to NO_2^- in a 1 m long copper-coated cadmium wire (CuCd) reduction column. NO_2^- was then reacted with an acidic sulphanilamide solution to form a diazonium ion complex. This reacts with α-naphthyl-ethylene-diamine-dihydrochloride (NEDD) to form a red azo dye (Griess reaction) which is determined spectrophotometrically at 540 nm (Hansen and Koroleff, 1999). NH_4^+ concentrations were determined by a salicylate/DTT method. NH_4^+ in samples was reacted with a di-chloro-*s*-triazine-2, 4, 6-trione sodium salt dihydrate (DTT) reagent and tri-sodium-citrate (TSC)/NaOH buffer at pH 10.6. Salicylate is then used as a source of the phenolic ring rather than phenol, and sodium nitroprusside acts as a coupling agent to yield the 'indephenol-blue' complex, which is detected spectrophotometrically at 630 nm.

3. Results and discussion

3.1. CDOM in the estuarine environment

Previous work raised the possibility that spectral CDOM absorbance and fluorescence properties may be affected by changes in salinity and water pH (e.g. Senesi, 1990; Zepp et al., 2004). We therefore investigated possible effects of estuarine pH and salinity changes in our study area on spectral CDOM characteristics. A range of artificial salinities was prepared from R. Tyne water to 0, 7, 14, 21, 28 and 35 using constituents according to Grasshoff et al. (1999) and measured for both absorbance and fluorescence. Throughout the salinity range a_{350} and $S_{290-350}$ showed no significant change with salinity, with standard deviations of ±0.05% and ±0.1% respectively. Fluorescence measurements of fluorophores A, H, T and B were also found to exhibit no significant change, with less than ±1% standard deviation across the salinity range. We therefore concluded that salinity effects on spectral CDOM characteristics are negligible for the surface waters encountered in this study.

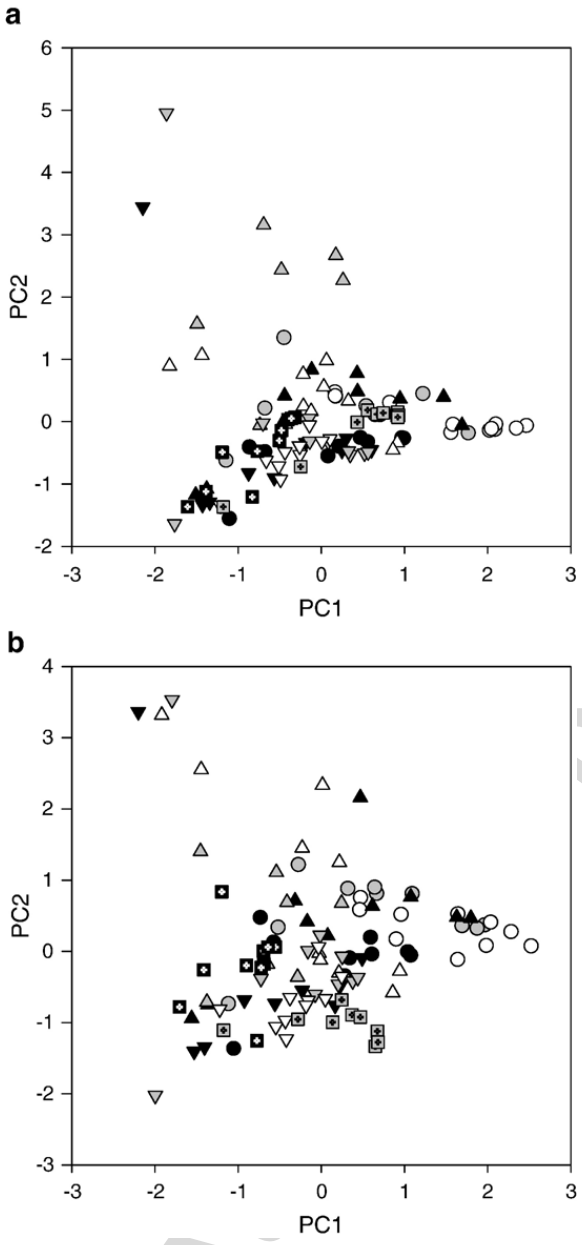

Fig. 4. Principal components analysis. (a) All Tyne and Tweed estuarine data (see Table 2 for component matrix and variance data). (b) Tyne and Tweed estuarine spectrophotometric data (see Table 3 for component matrix and variance data). Tyne data — black circles (11-07-2002), grey circles (31-07-2002), white circles (01-08-2002), black triangles (13-08-2002), grey triangles (04-10-2002), white triangles (03-03-2003), inverted black triangles (19-03-2003), inverted grey triangles (04-04-2003), inverted white triangles (23-07-2003). Tweed data — black squares, white spot (08-07-03), grey squares, black spot (03-12-03).

pH also varies across estuaries and typically ranges from 7.3 to 8.2 in the Tyne (Uher et al., 2001) and 7.3–8.8 in the Tweed. The comparatively higher pH of the Tweed estuary reflects carbonate rich groundwater inputs that dominate riverine dissolved inorganic carbon (DIC) during periods of low flow (Howland et al., 2000; Neal, 2002). Consistent with this higher pH values were observed in the Tweed summer transect (8.3–8.8) compared to the winter transect (7.3–8.1). Previous studies showed that pH changes may lead to small yet significant changes in CDOM spectral properties (Senesi, 1990; Mobed et al., 1996; Westerhoff et al., 2001). However, such studies tended to expose DOM to much wider pH ranges than those typically observed in estuarine waters, and pH induced variability over our estuarine pH range (7.3–8.8) was observed to be within analytical error (unpublished data). Therefore, samples in this study were not adjusted to constant pH values. Similarly, previous studies of CDOM across estuarine salinity gradients have not been adjusted to constant pH (De Souza Sierra et al., 1997; Del Castillo et al., 1999; Parlanti et al., 2000). In conclusion it was therefore found that neither salinity nor pH were responsible for the observed variability in CDOM spectral characteristics within the two estuaries.

3.2. Multivariate statistical analysis of Tyne and Tweed estuarine data

3.2.1. Principal components analysis

Principal components analysis may be seen as a method to simplify a data set by means of linear transformations that chose a new coordinate system in which the first axis (first principal component, PC1) describes the greatest variance within the dataset. The

second principal component accounts for the second greatest variance in the data and so on in decreasing order of magnitude. Such a statistical method is useful to investigate trends within the numerous parameters measured and to assess which parameters correlate to one another.

A principal components analysis was carried out on all the Tyne and Tweed estuarine data (Fig. 4a; Table 2). Principal component one (PC1) correlates strongly positively with fluorophore A and H I.U., a_{350}, DOC and fluorophore A and H emission wavelengths and strongly negatively with salinity, $S_{290-350}$ and fluorophore B I.U (Table 2). Therefore it is apparent that PC1 is correlated to estuarine mixing of riverine and marine waters. Principal component two (PC2) is correlated strongly positively with DON, TDN, NH_4^+ and fluorophore B and T I.U. and showed no strong negative relationship with any of the data (Table 2), and therefore it appears that it is correlated to nitrogen sources of pollution such as sewage. The results of the analysis (Table 2) demonstrate that 63.4% of the variability in the data can be explained by two sets of components with the first component alone explaining 43.1% of the variability.

From the principal components analysis there is clearly a relationship with river flow (Figs. 4a; 5), with samples taken at high river flow (e.g. 31-07-2002; 01-08-2002) exhibiting a stronger positive relationship on PC1 (Fig. 4a) as a result of their greater terrestrial character. The samples with the highest positive relationship on PC1 are those taken at the highest flow

Table 2
Principal components analysis of all Tyne and Tweed estuarine data; component matrix and variance data

Data	Component	
	1	2
Salinity	−0.836	−0.075
DOC (μM)	0.812	0.238
DON (μM)	−0.300	0.848
TDN (μM)	0.043	0.787
NH_4^+ (μM)	−0.204	0.787
$NO_3^-+NO_2^-$ (μM)	0.354	0.160
$S_{290-350}$ (nm^{-1})	−0.681	−0.232
a_{350} (m^{-1})	0.894	0.063
Fluorophore A Em.	0.632	−0.097
Fluorophore A I.U.	0.903	0.250
Fluorophore H Em.	0.727	0.176
Fluorophore H I.U.	0.927	0.140
Fluorophore B I.U.	−0.633	0.548
Fluorophore T I.U.	−0.391	0.566
% of Variance	43.1	20.3
Cumulative %	63.4	

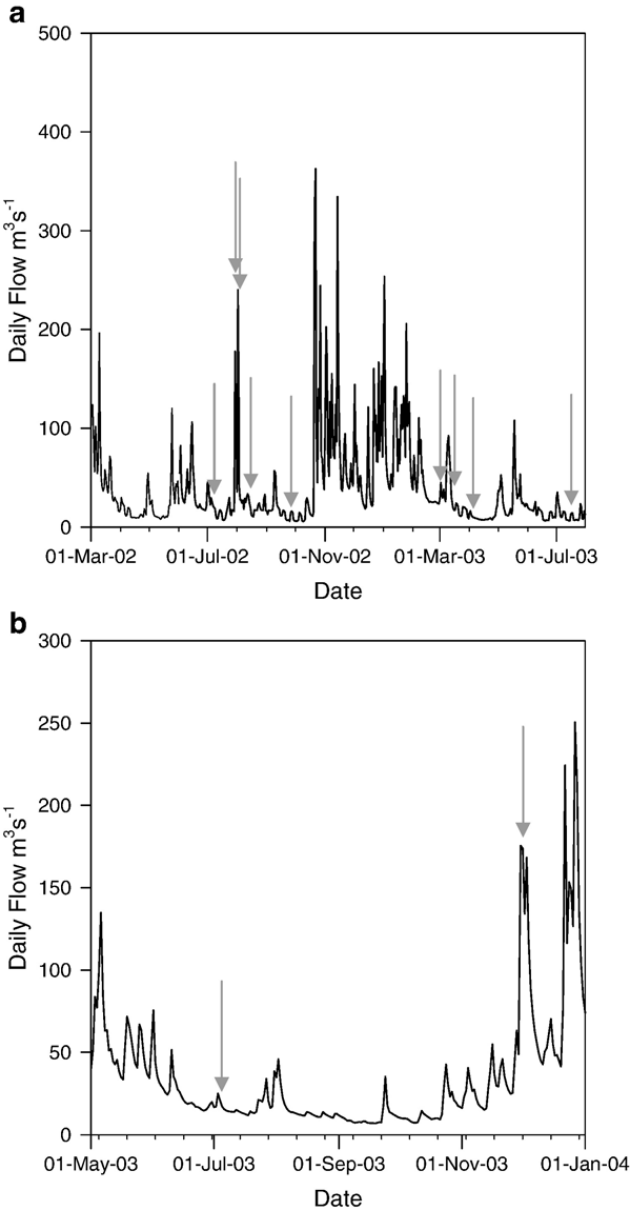

Fig. 5. Daily river discharge data: (a) River Tyne; (b) River Tweed. Sampling dates are indicated by arrows.

conditions in the Tyne estuary (31-07-2002; 01-08-2002) with the highest measured values in this study corresponding to positively correlating components on PC1 (Appendix A). PC2 positively highlights the data collected on the 04-10-2002 (grey triangles) from the Tyne estuary, which corresponds to the lowest river flow of all Tyne transects (Fig. 5a). This transect exhibited the highest estuarine levels of dissolved nitrogen in our data set (excluding Howdon STW) (Appendix A) most likely due to the lack of comparatively clean river water to dilute anthropogenic inputs at low flow. PC2 also positively highlights data from a number of other Tyne estuarine transects (31-07-2002; 03-03-2003; 19-03-

2003; 04-10-2003), which are observed to correspond to samples affected by Howdon STW. The two highest scoring samples on PC2 are both from the Howdon STW plume on 19-03-2003 and 04-10-2003, when of all the Tyne estuarine transects the highest values of measurements strongly correlated to PC2 were measured (Appendix A).

In order to test the potential of optical water characteristics alone for the discrimination and classification of estuarine waters, we carried out a second principal components analysis using solely our spectrophotometric measurements from both Tyne and Tweed estuaries (Fig. 4b; Table 3). PC1 was observed to correlate strongly positively with fluorophore A and H I.U., a_{350} and fluorophore A and H emission wavelengths, and negatively strongly with $S_{290–350}$ and fluorophore B I.U. (Table 3). Therefore, as for the principal components analysis of the whole data set, PC1 was correlated to the estuarine mixing of riverine and marine waters. PC2 was correlated strongly positively with fluorophore B and T I.U. and negatively strongly with none of the data (Table 3), and therefore it appears that PC2 was correlated to sources of pollution such as sewage, as was observed in the principal components analysis using the whole data set. As the use of only the spectrophotometric data results in PC1 and PC2 values that explain the same trends as the total data set, the potential of these measurements for investigating DOM dynamics is clear. The results of the second principal components analysis using solely the spectrophotometric data (Table 3) demonstrates that 74.9% of the variability in the data can be explained by two sets of components, with the first component alone explaining 56.4% of the variability.

As the principal components analysis based solely on the spectrophotometric data results in PC1 and PC2 explaining the same trends as the total data set it is unsurprising to see that the two data plots are similar (Fig. 4a+b). PC1 based on only spectrophotometric data is very similar to that observed in the whole data set with samples taken at high river flow (Fig. 5) exhibiting a stronger positive relationship on PC1 (Fig. 4b). Samples with the highest positive relationship on PC1 are those taken at the highest flow conditions in the Tyne estuary (31-07-2002; 01-08-2002; Fig. 5a), with the highest measured values in this study corresponding to positively correlating components on PC1 (Appendix A). PC2 however does not highlight the Tyne data collected on the 04-10-2002 (grey triangles) at the lowest river flow encountered of all Tyne transects as it does in the total data set on PC2 (Fig. 4a). This finding may be explained by the observation that the data collected on the 04-10-2002 were heavily affected by nitrogen pollution without showing elevated fluorophore B and T I.U. which are otherwise associated with anthropogenic inputs. Therefore with solely the spectrophotometric data those samples which score highly on PC2 (Fig. 4b) are those with high fluorophore B and T I.U. such as samples collected in the plume of Howdon STW or heavily impacted by polluted urban rivers.

To further examine the data set, it was subdivided into the respective subsets from the Tyne and Tweed estuaries and each subset was investigated by principal components analysis. For all data in both estuaries PC1 is observed to correlate to the estuarine mixing of riverine and marine waters (Tables 4 and 5). However

Table 3
Principal components analysis of all Tyne and Tweed estuarine spectrophotometric data; component matrix and variance data

Data	Component	
	1	2
$S_{290–350}$ (nm^{-1})	−0.697	−0.243
a_{350} (m^{-1})	0.894	0.173
Fluorophore A Em.	0.609	−0.301
Fluorophore A I.U.	0.925	0.280
Fluorophore H Em.	0.779	0.207
Fluorophore H I.U.	0.930	0.185
Fluorophore B I.U.	−0.623	0.689
Fluorophore T I.U.	−0.372	0.817
% of Variance	56.4	18.5
Cumulative %	74.9	

Table 4
Principal components analysis of all Tyne estuarine data; component matrix and variance data

Data	Component	
	1	2
Salinity	−0.888	−0.135
DOC (μM)	0.803	0.251
DON (μM)	−0.395	0.794
TDN (μM)	−0.186	0.939
NH_4^+ (μM)	−0.293	0.799
$NO_3^- + NO_2^-$ (μM)	0.466	0.499
$S_{290–350}$ (nm^{-1})	−0.704	−0.313
a_{350} (m^{-1})	0.886	0.075
Fluorophore A Em.	0.636	−0.054
Fluorophore A I.U.	0.893	0.262
Fluorophore H Em.	0.770	0.171
Fluorophore H I.U.	0.910	0.153
Fluorophore B I.U.	−0.633	0.575
Fluorophore T I.U.	−0.452	0.501
% of Variance	46.0	23.5
Cumulative %	69.5	

Table 5
Principal components analysis of all Tweed estuarine data; component matrix and variance data

Data	Component	
	1	2
Salinity	−0.813	−0.553
DOC (μM)	0.987	−0.114
DON (μM)	0.209	0.940
TDN (μM)	0.985	0.118
NH_4^+ (μM)	0.907	−0.198
$NO_3^-+NO_2^-$ (μM)	0.991	−0.004
$S_{290–350}$ (nm^{-1})	−0.478	−0.384
a_{350} (m^{-1})	0.987	−0.117
Fluorophore A Em.	0.781	−0.082
Fluorophore A I.U.	0.954	0.219
Fluorophore H Em.	0.868	0.071
Fluorophore H I.U.	0.993	−0.011
Fluorophore B I.U.	−0.804	0.332
Fluorophore T I.U.	−0.729	0.635
% of Variance	72.1	14.2
Cumulative %	86.3	

PC1 was observed to explain only 46.0% of the variability in the Tyne estuary compared to 72.1% in the Tweed estuary. This finding appears to highlight the anthropogenically impacted nature of the Tyne in comparison to the Tweed which does not suffer from the point source pollution observed in the Tyne. Consequently a higher percentage of data variability in the Tweed estuary is simply explained by the mixing of riverine and marine waters. PC2 for all Tyne estuarine data was observed to correlate with pollution derived nitrogen sources (Table 4) and explains 23.5% of the variability in the data. In contrast to the Tyne, the principal components analysis of the data subset from the Tweed indicated that PC2 explained 14.2% of the variability in the data. PC2 in the Tweed estuary showed a strong correlation with DON (Table 5). The significant correlation between DON and PC2 in the Tweed may be due to the release of DON-rich DOM from benthic macrophytes, which are widespread in the Tweed estuary but not in the Tyne (Appendix A).

If only the spectrophotometric data are considered for the principal components analysis of our data subsets for the Tyne and Tweed estuaries, PC1 is again correlated with estuarine mixing of riverine and marine waters (Tables 6 and 7). PC1 explained more of the variability in the Tweed estuary (71.6%) in comparison to the Tyne estuary (57.5%) presumably due to the impact of point sources of pollution in the Tyne estuary. In the Tyne estuary PC2 is correlated strongly positively with fluorophore B and T I.U. and negatively strongly with none of the data (Table 6), and therefore it appears that it is correlated to sources of pollution such as sewage, as

Table 6
Principal components analysis of all Tyne estuarine spectrophotometric data; component matrix and variance data

Data	Component	
	1	2
$S_{290–350}$ (nm^{-1})	−0.737	−0.325
a_{350} (m^{-1})	0.884	0.180
Fluorophore A Em.	0.608	−0.228
Fluorophore A I.U.	0.918	0.292
Fluorophore H Em.	0.801	0.109
Fluorophore H I.U.	0.916	0.208
Fluorophore B I.U.	−0.607	0.728
Fluorophore T I.U.	−0.459	0.794
% of Variance	57.5	18.6
Cumulative %	76.1	

with all the Tyne estuarine data and explains 18.6% of the variance in the data. PC2 in the Tweed estuary is strongly negatively correlated with $S_{290–350}$ and explains 12.6% of the variance in the data and appears to be explaining the variance in $S_{290–350}$ due to the sharp increase in S at higher salinities (Appendix A).

3.2.2. Discriminant analysis

The diagnostic value of the parameters in our data set with regard to the classification of estuarine waters was investigated further using discriminant analysis. The object of discriminant analysis is to allocate an individual sample to one of n groups based on the basis of its measurements or properties x (Mardia et al., 1977). Discriminant analysis is a two step process with the first step being the testing of significance of a set of discriminant functions and the second step being classification into groups. When there are several variables in a study the first step is to compare the matrix of total variances and covariances to the matrix of pooled within group variances and covariances. These two matrices are compared via multivariate F tests to determine if

Table 7
Principal components analysis of all Tweed estuarine spectrophotometric data; component matrix and variance data

Data	Component	
	1	2
$S_{290–350}$ (nm^{-1})	−0.458	−0.787
a_{350} (m^{-1})	0.986	−0.041
Fluorophore A Em.	0.825	−0.010
Fluorophore A I.U.	0.925	0.162
Fluorophore H Em.	0.853	0.190
Fluorophore H I.U.	0.983	0.018
Fluorophore B I.U.	−0.826	0.318
Fluorophore T I.U.	−0.797	0.476
% of Variance	71.6	12.6
Cumulative %	84.2	

there are any significant differences (with respect to all variables) between the groups. This first step is the same as calculating the multivariate analysis of variance (MANOVA). If the group means are found to be statistically significant the classification of variables is carried out. Discriminant analysis automatically determines an optimal combination of variables so function one provides the most overall discrimination between groups, function two provides the second most, etc. Furthermore, the functions are orthogonal to one another and so their contributions to the discrimination between groups do not overlap (i.e. function one describes the most variation; function two describes the largest part of the unexplained variation, etc.). A canonical correlation analysis is undertaken which determines the successive functions and canonical roots, and samples are classified into the groups where they have the highest classification score as classification is possible from the canonical functions.

The individual sample groups were classified according to salinity and sample site collection. Group 1, Tyne freshwater samples (R. Tyne); group 2, Tyne samples with a salinity greater than freshwater but less than 32.0 (Tyne estuary); group 3, all samples with a salinity greater than 32.0 (coastal North Sea); group 4, samples collected from the plume of the Howdon STW (sewage); group 5, samples collected from urban river impacted sites (poor water quality rivers); group 6, Tweed samples with a salinity greater than freshwater but less than 32.0 (Tweed estuary); group 7, Tweed freshwater samples (R. Tweed).

The results of the discriminant analysis show that 59.8% of the original groups are correctly classified for all the Tyne and Tweed estuarine data (Tables 8, 9 and Fig. 6a). Discriminant function 1 explains 61.4% of the variance and shows the strongest negative correlation to $NO_3^- + NO_2^-$ and the strongest positive correlation to fluorophore H emission wavelength (Table 8 and Fig. 6a). Discriminant function 1 discriminates between the Tyne and Tweed estuaries due to the higher $NO_3^- + NO_2^-$ load of the Tweed (Appendix A), and the emission wavelength of fluorophore H which typically exhibits a bathochromic shift in the Tyne estuary in comparison to the Tweed estuary (Appendix A). Discriminant function 2 explains a further 27.9% of the variance and correlates positively with fluorophore A I.U., $NO_3^- + NO_2^-$ and fluorophore H emission wavelength, and negatively with $S_{290-350}$. Discriminant function 2 shows the transition between riverine and marine endmembers and shows which variables highlight the differences between these endmembers. $S_{290-350}$ and fluorophore H emission wavelength both show clear shifts at high salinities (Appendix A) and so have clear potential for defining the marine endmember. Fluorophore A I.U. and $NO_3^- + NO_2^-$ are two of the most linear tracers of conservative mixing of all the variables measured (Appendix A). Hence they show the most consistent differences between estuarine sites and therefore a high potential for discrimination. Discriminant function 3 (Table 8; not shown on Fig. 6a) is positively correlated with fluorophore B and T I.U., NH_4^+, DON and TDN and so is likely correlated to anthropogenic inputs (groups 4 and 5).

Overall, group classification by the discriminant analysis presented here varies from 50 to 100% (Table 9). Only one group, coastal North Sea water is discriminated 100% as a result of its unique spectrophotometric features (discriminant function 2) (Fig. 6a; Table 8). Discriminant function 1 is clearly good at distinguishing between the two estuaries as there is no

Table 8
Discriminant analysis functions for all Tyne and Tweed estuarine data; structure matrix

Data	Function		
	1	2	3
DOC (μM)	0.188	0.261	−0.284
DON (μM)	0.073	0.032	0.635
TDN (μM)	−0.123	0.304	0.540
NH_4^+ (μM)	0.187	0.018	0.662
$NO_3^- + NO_2^-$ (μM)	−0.426	0.519	−0.030
$S_{290-350}$ (nm^{-1})	−0.076	−0.639	0.077
a_{350} (m^{-1})	0.135	0.296	−0.421
Fluorophore A Em.	0.014	0.467	−0.260
Fluorophore A I.U.	0.234	0.533	−0.275
Fluorophore H Em.	0.374	0.503	−0.247
Fluorophore H I.U.	0.151	0.387	−0.394
Fluorophore B I.U.	−0.026	−0.197	0.872
Fluorophore T I.U.	0.143	−0.139	0.579
% of Variance	61.4	27.9	7.1

Table 9
Discriminant analysis functions for all Tyne and Tweed estuarine data; classification results

Group	*n*	Predicted group membership (%)						
		1	2	3	4	5	6	7
1	11	**54.5**	18.2	0	0	27.3	0	0
2	50	16.0	**50.0**	2.0	2.0	30.0	0	0
3	13	0	0	**100**	0	0	0	0
4	10	0	30.0	0	**60.0**	10.0	0	0
5	6	0	33.3	0	16.7	**50.0**	0	0
6	12	0	0	8.3	0	0	**66.7**	25
7	5	0	0	0	0	0	40.0	**60.0**

1. R. Tyne; **2.** Tyne estuary; **3.** coastal North Sea; **4.** Howdon STW; **5.** Tyne estuarine urban river impacted sites; **6.** Tweed estuary; **7.** R. Tweed.

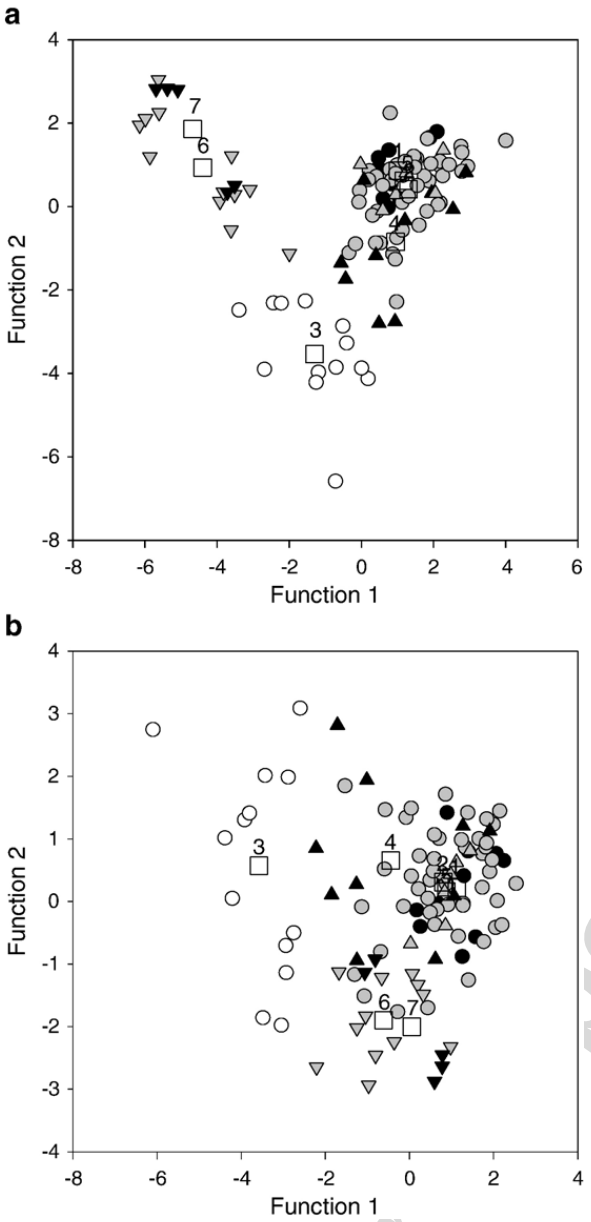

Fig. 6. Discriminant analysis functions. (a) All Tyne and Tweed estuarine data (see Tables 8 and 9 for structure matrix and classification results). (b) Tyne and Tweed estuarine spectrophotometric data (see Tables 10 and 11 for structure matrix and classification results). 1. R. Tyne (black circles); 2. Tyne estuary (grey circles); 3. coastal North Sea (white circles); 4. Howdon STW (black triangles); 5. Tyne estuarine urban river impacted sites (grey triangles); 6. Tweed estuary (inverted grey triangles); 7. R. Tweed (inverted black triangles). Numbered white squares (1–7) represent group centroids.

overlap between any R. Tyne/Tyne estuarine and R. Tweed/Tweed estuarine samples. Significant overlap between groups is observed primarily as a result of attempting to classify between riverine and estuarine measurements. Group 1 (R. Tyne) is classified correctly 54.5% and group 2 (Tyne estuary) is classified correctly 50.0% with 18.2% of incorrectly classified group 1 falling in group 2 and 16.0% of incorrectly classified group 2 falling in group 1 (Table 9). Group 7 (R. Tweed) exhibits a similar pattern with 60% classified correctly and with 40.0% of incorrectly classified group 7 falling in group 6 (Tweed estuary). Group 6 is correctly classified 66.7% and 25% of incorrectly classified group 6 falls in group 7. This overlap between groups 6 and 7 (i.e. Tweed river and estuary) most likely reflected the low variability in the diagnostic parameters $S_{290-350}$ and fluorophore H emission maxima below salinity 28 (Appendix A). Fluorophore A I.U. and $NO_3^- + NO_2^-$ showed more pronounced variability at salinities below 28, and were therefore of more diagnostic value for discriminating riverine and estuarine waters. However, differences in river input also caused large changes in fluorophore A I.U. and $NO_3^- + NO_2^-$, leading to significant overlap between riverine and estuarine data (Fig. 5).

Overlap between groups was also observed between R. Tyne/Tyne estuarine samples and the anthropogenically impacted groups (4 and 5). 30.0% of Tyne estuarine samples (group 2) were incorrectly classified into group 5 (urban river impacted sites) and 33.3% of group 5 were incorrectly classified into group 2 (estuarine), showing significant overlap between these two groups. This finding is unsurprising as the discharge from polluted urban rivers affects not only estuarine waters directly at their mouths (i.e. those classified as group 5) but also other estuarine areas dependent on tidal mixing and dispersion. However, mixing and dispersion were not considered in our classification scheme. In addition, at high river input (Fig. 5a) the signal from the polluted urban rivers is masked by and diluted by the river input. Consistent with this, at low river flow (Fig. 5a) 27.3% of group 1 (R. Tyne) is classified as group 5. Group 4 (Howdon STW) is correctly classified 60% with 30% being incorrectly classified as group 2 (Tyne estuary) and 10% as group 5 (urban river impacted sites). This misclassification is due to changes in river input (Fig. 5a), but also to variations in the rate of Howdon STW discharge with time. 2.0% of group 2 is incorrectly classified as group 4 due to one sample taken adjacent to the Howdon STW plume at low river flow, which is clearly impacted by the Howdon STW plume. Although group 3 (coastal North Sea) is correctly classified 100%, 2.0% of group 2 (Tyne estuary) and 8.3% of group 6 (Tweed estuary) are incorrectly classified as group 3. In both cases this is due to one sample taken at low river flow and high salinities, which exhibits either the shift in $S_{290-350}$ or fluorophore H emission typical of marine waters (Fig. 5a;

Appendix A) (Blough and Del Vecchio, 2002; Coble, 1996; Del Castillo et al., 1999).

As with our principal components analysis described above, we carried out a second discriminate function analysis on a data subset containing only spectral CDOM characteristics. The results from this analysis showed that 53.3% of the original groups are correctly classified for all the Tyne and Tweed estuarine data (Tables 10, 11 and Fig. 6b). Discriminant function 1 explained 60.0% of the variance and showed the strongest positive correlation to fluorophore H emission and fluorophore A I.U. and the strongest negative correlation to $S_{290-350}$ (Table 10 and Fig. 6b). Discriminant function 1 discriminated between terrestrial and marine waters due to the shift in $S_{290-350}$ and fluorophore H emission wavelength typical of marine waters (Blough and Del Vecchio, 2002; Coble, 1996; Del Castillo et al., 1999). Furthermore discriminant function 1 showed a stronger correlation with fluorophore A I.U. than with fluorophore H I.U. (Table 10) and fluorophore H I.U. was observed to have greater variability than fluorophore A I.U. in both marine and riverine waters (Appendix A). Therefore, we concluded that fluorophore A I.U. is of higher diagnostic value for discriminating between riverine and marine samples.

Discriminant function 2 explains a further 20.7% of the variance and correlates positively with fluorophore T I.U. and fluorophore H emission wavelength (Table 10). Discriminant function 2 discriminates between the two estuaries (Tyne and Tweed) due to the emission wavelength of fluorophore H, which typically exhibits a bathochromic shift in the Tyne estuary in comparison to the Tweed estuary (Appendix A), and the higher fluorophore T I.U. observed in the Tyne estuary (Appendix A). Discriminant function 3 (Table 10; not shown on Fig. 6b) is positively correlated with fluorophore B and T I.U. and so is likely correlated with anthropogenic inputs (groups 4 and 5).

Table 10
Discriminant analysis functions for all Tyne and Tweed estuarine spectrophotometric data; structure matrix

Data	Function		
	1	2	3
$S_{290-350}$ (nm^{-1})	−0.605	0.356	0.078
a_{350} (m^{-1})	0.353	0.072	−0.471
Fluorophore A Em.	0.412	−0.338	−0.293
Fluorophore A I.U.	0.627	0.089	−0.304
Fluorophore H Em.	0.699	0.402	−0.259
Fluorophore H I.U.	0.443	0.030	−0.438
Fluorophore B I.U.	−0.190	0.104	0.938
Fluorophore T I.U.	−0.020	0.431	0.615
% of Variance	60.0	20.7	12.6

Table 11
Discriminant analysis functions for all Tyne and Tweed estuarine spectrophotometric data; classification results

Group	*n*	Predicted group membership (%)						
		1	2	3	4	5	6	7
1	11	**54.5**	18.2	0	0	27.3	0	0
2	50	16.0	**36.0**	2.0	6.0	30.0	6.0	4.0
3	13	0	0	**76.9**	7.7	0	15.4	0
4	10	0	20.0	0	**60.0**	10.0	10.0	0
5	6	0	33.3	0	0	**66.7**	0	0
6	12	0	0	0	0	0	**83.3**	16.7
7	5	0	0	0	0	0	40.0	**60.0**

1. R. Tyne; **2.** Tyne estuary; **3.** coastal North Sea; **4.** Howdon STW; **5.** Tyne estuarine urban river impacted sites; **6.** Tweed estuary; **7.** R. Tweed.

Group classification by the discriminant analysis using spectrophotometric data varies from 36.0 to 83.3%. As observed with the complete data set, significant overlap between groups is observed as a result of attempting to classify between riverine and estuarine measurements. Group 1 (R. Tyne) is classified correctly 54.5% and group 2 (Tyne estuary) is classified correctly 36.0% with 18.2% of incorrectly classified group 1 falling in group 2 and 16.0% of incorrectly classified group 2 falling in group 1 (Table 11). Group 7 (R. Tweed) exhibits a similar pattern with 60% classified correctly and with 40.0% of incorrectly classified group 7 falling in group 6 (Tweed estuary). Group 6 is correctly classified 83.3% and 16.7% of incorrectly classified group 6 falls in group 7. This overlap reflects the relative constancy in $S_{290-350}$ and fluorophore H emission wavelength below salinity 28 resulting in fluorophore H I.U. becoming diagnostically important. Hence the overlap between riverine and estuarine samples is a result of the changes in fluorophore H I.U. as a consequence of differences in river input (Fig. 5; Appendix A). Overlap between groups is also observed between R. Tyne/Tyne estuarine samples and the anthropogenically impacted groups (4 and 5). 30.0% of Tyne estuarine samples (group 2) are incorrectly classified as group 5 (urban river impacted sites) and 33.3% of group 5 is incorrectly classified as group 2 showing significant overlap between these two groups. This overlap is unsurprising as the polluted urban rivers impact on the estuary and only the samples taken at their mouths were classified as group 5 in the discriminant analysis. As mentioned previously this does not allow for dispersion processes and also at high river input (Fig. 5a) the signal from the polluted urban rivers is masked by and diluted by the river input. This is further evidenced as at low riverine flow (Fig. 5a) 27.3% of group 1 (R. Tyne) is classified as group 5.

Group 4 (Howdon STW) is correctly classified 60% with 20% being incorrectly classified as group 2 (Tyne estuary), 10% as group 5 (urban river impacted sites) and 10% as group 6 (Tweed estuary). Misclassification relating to group 4 is due to changes in river input (Fig. 5a), but also to variations in the Howdon STW discharge with time and load and the optical similarity between the Howdon STW plume and Tweed high salinity estuarine waters, particularly on the summer transect (08-07-2003). The optical similarity between the Howdon STW plume on the one hand and coastal North Sea and Tweed estuarine water on the other is further illustrated by the finding that 15.4% of group 3 (coastal North Sea) was incorrectly classified into group 6 (Tweed estuary) and that a further 7.7% were incorrectly classified into group 4 (Howdon STW). On a number of occasions the discharge from Howdon STW shows optical similarity to marine and high salinity waters particularly due to high fluorophore B and T I.U. and a hypsochromic shift in fluorophores A and H emission maxima. Therefore it appears that the Howdon STW plume is optically difficult to separate from high salinity waters, thus resulting in the incorrect group classifications. 6.0% of group 2 is incorrectly classified as group 4 due to this difficulty in discrimination between the Howdon STW plume and high salinity estuarine waters, and samples taken adjacent to the Howdon STW plume at low river flow which are clearly impacted by it.

In the discriminant analysis carried out on the entire data set, no Tyne estuarine samples were classified as Tweed and vice versa. However in the discriminant analysis using only spectrophotometric data 6.0% of group 2 (Tyne estuary) are classified as group 6 (Tweed estuary) and 4% of group 2 are classified as group 7 (R. Tweed). The incorrectly classified data are all from low river input Tyne transects when the Tyne terrestrial component is more similar to that observed in the Tweed. 2.0% of group 2 is incorrectly classified as group 3 and this is due to one sample taken at salinity ~26.0 on 11-07-2002 that exhibited a typically marine value for $S_{290-350}$ (Appendix A).

4. Conclusion

The results of our multivariate analyses indicate that spectrophotometric techniques may be valuable in the discriminatory classification of water bodies. In particular, the spectral slope parameter, $S_{290-350}$, the wavelength of the fluorophore H emission maxima and fluorophores T and B intensities appeared to be valuable diagnostics in the classification of estuarine waters. Our results indicate that spectrophotometric data alone are able to discriminate to a high degree between riverine, marine and anthropogenically affected waters on the basis of CDOM diagnostics. However, spectrophotometric data alone were less well suited to distinguishing between the Tyne and Tweed estuaries, because differences in nutrient loadings were more pronounced than differences in spectral CDOM characteristics alone. In particular, the high $NO_3^- + NO_2^-$ loading of the Tweed estuary proved a good discriminator. The Tyne and Tweed estuaries, however, showed significant differences in the emission wavelengths of the fluorophore H maximum, and fluorophore T I.U. were significantly higher in the Tyne than they were in the Tweed. Fluorophore H emission in the Tyne estuary generally occurred at longer wavelengths as compared to those observed in the Tweed estuary (Appendix A), with the emission maximum of fluorophore H in the Tyne freshwater endmember ranging from 436 to 445.5 nm (mean=441 nm, $n=7$) compared to a range of 420.5–429 (mean=425 nm, $n=2$) in the Tweed freshwater endmember. Such a bathochromic shift in emission maxima may be attributed to an increase in lower energy transitions consistent with an increase in DOM aromaticity (Coble, 1996). Similarly, other workers attributed bathochromic shifts in fluorophore H to DOM degradation state and age (Senesi et al., 1991; Parlanti et al., 2000).

It is apparent from the discriminant analyses (Tables 8 and 10) that the fluorophore H emission maximum is also diagnostically important in discriminating marine DOM from terrestrially or anthropogenically derived material. The hypsochromic shift in fluorophore H emission wavelengths at salinities >25 observed in this study in both Tyne and Tweed estuaries was similar to previous observations and was also consistent with a decrease in aromaticity with increasing salinity (Coble, 1996; De Souza Sierra et al., 1997; Del Castillo et al., 1999). It has been suggested that such a hypsochromic shift may be attributed to the photochemical and microbial degradation of terrigenous DOM, its mixing with a marine form of DOM, which is less aromatic in nature, or a combination of these processes (Coble, 1996; Blough and Del Vecchio, 2002). The sudden hypsochromic shift in fluorophore H emission wavelengths observed towards higher salinities may be explained by the mixing of a CDOM rich riverine endmember with a dilute marine endmember. Given the pronounced CDOM concentration differences between riverine and marine waters, the characteristics of the marine endmember would be expected to emerge only towards high salinities, when the marine fluorophores become dominant

(De Souza Sierra et al., 1997). A sudden hypsochromic shift at high salinities may also be due to shading from CDOM and high turbidity at low to mid-salinities; hence photochemical degradation will occur only at high salinities due to the decrease in light attenuation (Del Castillo et al., 1999).

In conjunction with the wavelength of fluorophore H emission maxima, spectral slope, $S_{290–350}$, also proved valuable in discriminating between waters with different levels of marine vs. terrestrial CDOM. Several possible processes have been postulated in order to account for an increase in S towards high salinities as described in this study, namely mixing between distinct end members, photochemical and microbial degradation (Green and Blough, 1994; Blough and Del Vecchio, 2002). However, $S_{290–350}$ was not particularly well suited to distinguishing between the Tyne and Tweed estuaries (Table 8), and was only the third most important discriminator in our discriminant function analysis based on the spectrophotometric data alone (Table 10). The strongest parameter for distinguishing between the Tyne and Tweed estuaries spectrophotometrically was fluorophore T I.U. with the Tyne having much higher fluorophore T intensity compared to that observed in the Tweed. Previous studies have indicated fluorophore T to be associated with protein-like fluorescence of sewage affected waters (Baker, 2002a,b; Baker et al., 2003), indicating the anthropogenically impacted nature of the Tyne estuary.

Our study suggests that it may be possible to classify estuarine waters into distinct groups (e.g. terrestrial, sewage and marine) with characteristic CDOM spectral properties and to distinguish between waters derived from different catchments (Tyne and Tweed) based on their optical properties. Given the recent advances in spectrophotometric techniques, particularly the high spatio-temporal resolution of available in-situ instrumentation (Chen and Gardner, 2004) the application of optical techniques and multivariate statistics in the biogeochemical classification of estuarine waters seems promising. While currently available instrumentation for in-situ measurements of CDOM absorbance and fluorescence is as yet largely limited to individual wavelengths, they already open up the prospect of targeting optical parameters identified as particularly useful in laboratory studies. Optical parameters with diagnostic value in the characterisation of DOM origin such as the spectral slope parameter, $S_{290–350}$, the spectral position of fluorophore H emission maximum, and fluorophores T and B intensities therefore have the potential to develop into valuable tools in the near future. For example, our results indicate that fluorophore T and B intensities correspond to high TDN, DON and NH_4^+ (Tables 2, 4, and 8) and therefore have potential for tracing sewage and other human and agricultural derived wastes. Spectral slope and the position of the fluorophore H emission maximum were clearly useful at discriminating DOM.

As the fluorophore H emission maximum is believed to exhibit a bathochromic shift with increasing DOM aromaticity (Coble, 1996), it may be used to distinguish between catchments (Tables 8 and 10) which display differences in DOM aromaticity. Furthermore, fluorophore H emission characteristics have potential for monitoring of drinking water extractions in freshwaters as aromaticity has been linked to production of carcinogens on chlorination such as trihalomethanes (Fleck et al., 2004; Nikolaou et al., 2004). In addition, the techniques described here may be utilised in monitoring DOC export and determining the source of the organic matter under different river regimes and therefore improve our understanding in the mid and high latitude regions where riverine DOC loads are increasing (Worrall et al., 2004; Bellamy et al., 2005). Finally as the discriminant analysis with solely the spectrophotometric techniques shows little overlap between the two estuaries it further highlights the potential of these techniques for estuarine fingerprinting with respect to ballast water uptake and pollution (Hall et al., 2005). Therefore with advances in spectrophotometer technology that include the possibility of in situ and real-time spectral slope measurements from submersible UV–Vis spectrophotometers, and portable luminescence spectrophotometers that can determine wavelength variations of fluorophore H emission maxima, these techniques have the potential to become a powerful and diagnostic approach within the environmental sciences.

Acknowledgements

We thank the captain and crew of RV *Bernicia*, J. Barnes, A. Pike and Steve Mowbray for help with field sampling. Helpful comments were provided by V. Kitidis and A. Stubbins and R. Inverarity (Environment Agency, Newcastle-upon-Tyne) kindly provided River Tyne flow data. Thanks to E. Achterberg and E. Badr at the University of Plymouth and D. Purdie and J. Homewood at Southampton Oceanography Centre for assistance and use of their HTCOs for DOC/TDN analyses. This work was supported by the U.K. Natural Environmental Research Council through the GANE thematic programme (Grant Number NER/T/S/2000/00186 awarded to G. Uher and R.C. Upstill-Goddard (Newcastle) and R.S. Ganeshram and G.L. Cowie (Edinburgh).

Appendix A. Supplementary Data

Supplementary data associated with this article can be found, in the online version, at doi:10.1016/j.scitotenv.2006.10.052.

References

Alberts JJ, Takacs M, Schalles J. Ultraviolet–visible and fluorescence spectral evidence of natural organic matter (NOM) changes along an estuarine salinity gradient. Estuaries 2004;27(2):296–310.

Baker A. Fluorescence excitation–emission matrix characterization of some sewage impacted rivers. Environ Sci Technol 2001;35:948–53.

Baker A. Fluorescence properties of some farm wastes: implications for water quality monitoring. Water Res 2002a;36:189–95.

Baker A. Fluorescence excitation–emission matrix characterisation of river waters impacted by a tissue mill effluent. Environ Sci Technol 2002b;36(7):1377–82.

Baker A. Thermal fluorescence quenching properties of dissolved organic matter. Water Res 2005;39:4405–12.

Baker A, Inverarity R. Protein-like fluorescence intensity as a possible tool for determining river water quality. Hydrol Process 2004;18(15):2927–45.

Baker A, Inverarity R, Charlton ME, Richmond S. Detecting river pollution using fluorescence spectrophotometry: case studies from the Ouseburn, NE England. Environ Pollut 2003;124:57–70.

Bashford CL, Harris DA. Spectrophotometry and spectrofluorimetry: a practical approach. Oxford: IRL Press; 1987.

Bellamy PH, Loveland PJ, Bradley RI, Lark RM, Kirk GJD. Carbon losses from all soils across England and Wales 1978–2003. Nature 2005;437:245–8.

Blough NV, Del Vecchio R. Chromophoric DOM in the Coastal Environment. In: Hansell DA, Carlson CA, editors. Biogeochemistry of Marine Dissolved Organic Matter. Academic Press; Elsevier Science, San Diego, 2002. pp. 509–546.

Blough NV, Green SA. Spectroscopic characterization and remote sensing of NLOM. In: Zepp RG, Sonntag C, editors. The role of non-living organic matter in the Earth's Carbon cycle. NYC: John Wiley and Sons; 1995. p. 23–45.

Blough NV, Zafiriou OC, Bonilla J. Optical absorption spectra of water from the Orinoco River outflow: terrestrial input of colored organic matter to the Caribbean. J Geophys Res 1993;98:2271–8.

Bricaud A, Morel A, Prieur L. Absorption by dissolved organic matter of the sea (yellow substance) in the UV and visible domains. Limnol Oceanogr 1981;26(1):43–53.

Chen RF, Gardner GB. High-resolution measurements of chromophoric dissolved organic matter in the Mississippi and Atchafalaya River plume regions. Mar Chem 2004;89:103–25.

Coble PG. Characterization of marine and terrestrial DOM in seawater using excitation–emission matrix spectroscopy. Mar Chem 1996;51:325–46.

Coble PG, Green SA, Blough NV, Gagosian RB. Characterization of dissolved organic matter in the Black Sea by fluorescence spectroscopy. Nature 1990;348:432–5.

Coble PG, Schultz CA, Mopper K. Fluorescence contouring analysis of DOC intercalibration experiment samples: a comparison of techniques. Mar Chem 1993;41:173–8.

De Souza Sierra MM, Donard OFX, Lamotte M, Belin C, Ewald M. Fluorescence spectroscopy of coastal marine waters. Mar Chem 1994;47:127–44.

De Souza Sierra MM, Donard OFX, Lamotte M. Spectral identification and behaviour of dissolved fluorescent material during estuarine mixing processes. Mar Chem 1997;58:51–8.

Del Castillo CE, Coble PG, Morell JM, Lopez JM, Corredor JE. Analysis of the optical properties of the Orinoco River plume by absorption and fluorescence spectroscopy. Mar Chem 1999;66:35–51.

Del Vecchio R, Blough NV. Spatial and seasonal distribution of chromophoric dissolved organic matter and dissolved organic carbon in the Middle Atlantic Bight. Mar Chem 2004;89(1–4):169–87.

Dittmar T, Kattner G. The biogeochemistry of the river and shelf ecosystem of the Arctic Ocean: a review. Mar Chem 2003;83:103–20.

Elliot S, Lead JR, Baker A. Characterisation of the fluorescence from freshwater, planktonic bacteria. Water Res 2006;40:2075–83.

Ferrari GM, Dowell MD, Grossi S, Targa C. Relationship between the optical properties of chromophoric dissolved organic matter and total concentration of dissolved organic carbon in the southern Baltic Sea region. Mar Chem 1996;55:299–316.

Fleck JA, Bossio DA, Fuji R. Dissolved organic carbon and disinfection by-product precursor release from managed peat soils. J Environ Qual 2004;33:465–75.

Fox IA, Johnson RC. The hydrology of the River Tweed. Sci Total Environ 1997;194:163–72.

Grasshoff K, Kremling K, Ehrhardt M. Methods of seawater analysis. Weinheim: Wiley-VCH; 1999.

Green SA, Blough NV. Optical absorption and fluorescence properties of chromophoric dissolved organic matter in natural waters. Limnol Oceanogr 1994;39(8):1903–16.

Hall GJ, Clow KE, Kenny JE. Estuarial fingerprinting through multidimensional fluorescence and multivariate analysis. Environ Sci Technol 2005;39(19):7560–7.

Hansen HP, Koroleff F. Determination of nutrients. In: Grasshoff K, Kremling K, Ehrhardt M, editors. Methods of seawater analysis. 3rd edition. Wiley; 1999.

Hart SJ, Jiji RD. Light emitting diode excitation emission fluorescence spectroscopy. Analyst 2002;127:1693–9.

Hedges JI, Keil RG. Organic geochemical perspectives on estuarine processes: sorption reactions and consequences. Mar Chem 1999;65:55–65.

Hedges JI, Keil RG, Benner R. What happens to terrestrial organic matter in the ocean? Org Geochem 1997;27:195–212.

Holbrook RD, Yen JH, Grizzard TJ. Characterizing natural organic material from the Occoquan Watershed (Northern Virginia, US) using fluorescence spectroscopy and PARAFAC. Sci Total Environ 2006;361:249–66.

Howland RJM, Tappin AD, Uncles RJ, Plummer DH, Bloomer NJ. Distributions and seasonal variability of pH and alkalinity in the Tweed Estuary, U.K. Sci Total Environ 2000;251:125–38.

Kitidis V, Stubbins AP, Uher G, Upstill-Goddard RC, Law CS, Woodward EMS. Variability of Chromophoric Organic Matter in surface waters of the Atlantic Ocean. Deep Sea Research Pt. II 2006;53:1666–84.

Kowalczuk P, Cooper WJ, Whitehead RF, Durako MJ, Sheldon W. Characterization of CDOM in an organic-rich river and surrounding coastal ocean in the South Atlantic Bight. Aquat Sci 2003;65:384–401.

Mardia KV, Kent JT, Bibby JM. Multivariate analysis. NYC: Academic Press; 1977.

McKnight DM, Boyer EW, Westerhoff PK, Doran PT, Kulbe T, Andersen DT. Spectrofluorometric characterization of aquatic

fulvic acids for determination of precursor organic material and general structural properties. Limnol Oceanogr 2001;46:38–48.
Mobed JJ, Hemmingsen SL, Autry JL, McGown LB. Fluorescence characterisation of IHSS Humic Substances: total luminescence spectra with absorbance correction. Environ Sci Technol 1996;30: 3061–6.
Mopper K, Schultz CA. Fluorescence as a possible tool for studying the nature and water column distribution of DOC components. Mar Chem 1993;41:229–38.
Morris AW, Mantoura RFC, Bale AJ, Howland RJM. Very low salinity regions of estuaries: important sites for chemical and biological reactions. Nature 1978;274:678–80.
Neal C. Calcite saturation in eastern U.K. rivers. Sci Total Environ 2002;282:311–26.
Nikolaou AD, Golfinopoulos SK, Arhonditsis GB, Kolovoyiannis V, Lekkas TD. Modeling the formation of chlorination by-products in river waters with different quality. Chemosphere 2004;55:409–20.
Ohno T. Fluorescence inner-filtering correction for determining the humification index of dissolved organic matter. Environ Sci Technol 2002;36(4):742–6.
Parlanti E, Worz K, Geoffrey L, Lamotte M. Dissolved organic matter fluorescence spectroscopy as a tool to estimate biological activity in a coastal zone submitted to anthropogenic inputs. Org Geochem 2000;31:1765–81.
Patel-Sorrentino N, Mounier S, Benaim JY. Excitation–emission fluorescence matrix to study pH influence on organic matter fluorescence in the Amazon Basin rivers. Water Res 2002;36: 2571–81.
Robson AJ, Neal C. Regional water quality of the River Tweed. Sci Total Environ 1997;194:173–92.
Senesi N. Molecular and quantitative aspects of the chemistry of fulvic acid and its interactions with metal ions and organic chemicals. Anal Chim Acta 1990;232(1):77–106.
Senesi N, Miano TM, Provenzano MR, Brunetti G. Characterization, differentiation and classification of humic substances by fluorescence spectroscopy. Soil Sci 1991;152:259–71.
Skoog A, Wedgorg M, Fogelqvist E. Photobleaching of fluorescence and the organic carbon concentration in a coastal marine environment. Mar Chem 1996;55:333–45.
Stedmon CA, Markager S. Resolving the variability in dissolved organic matter fluorescence in a temperate estuary and its catchment using PARAFAC analysis. Limnol Oceanogr 2005;50:686–97.
Stedmon CA, Markager S, Kaas H. Optical properties and signatures of chromophoric dissolved organic matter (CDOM) in Danish coastal waters. Estuar Coast Shelf Sci 2000;51(2):267–78.
Stedmon CA, Markager S, Bro R. Tracing dissolved organic matter in aquatic environments using a new approach to fluorescence spectroscopy. Mar Chem 2003;82:239–54.
Stubbins AP. Aspects of aquatic CO photoproduction from CDOM. PhD thesis In: Marine sciences and coastal management. Newcastle-upon-Tyne, Newcastle, 2001. pp. 201.
Twardowski MS, Boss E, Sullivan JM, Donaghay PL. Modeling the spectral shape of absorption by chromophoric dissolved organic matter. Mar Chem 2004;89:69–88.
Uher G, Andreae MO. The diel cycle of carbonyl sulfide in marine surface waters: field study results and a simple model. Aquat Geochem 1997;2:313–44.
Uher G, Hughes C, Henry G, Upstill-Goddard RC. Non-conservative mixing behaviour of colored dissolved organic matter in a humic-rich turbid estuary. Geophys Res Lett 2001;28(17):3309–12.
Uncles RJ, Stephens JA. Salt intrusion in the Tweed Estuary. Estuar Coast Shelf Sci 1996;43(3):271–93.
Vodacek A. An explanation of the spectral variation in freshwater CDOM fluorescence. Limnol Oceanogr 1992;37:1808–13.
Vodacek A, Hoge FE, Swift RN, Yungel JK, Peltzer ET, Blough NV. The use of in situ airborne fluorescence measurements to determine UV absorption coefficients and DOC concentrations in surface waters. Limnol Oceanogr 1995;40:411–5.
Vodacek A, Blough NV, DeGrandpre MD, Peltzer ET, Nelson RK. Seasonal variation of CDOM and DOC in the Middle Atlantic Bight: terrestrial inputs and photooxidation. Limnol Oceanogr 1997;42:674–86.
Walsh TW. Total dissolved nitrogen in seawater: a new-high-temperature combustion method and a comparison with photo-oxidation. Mar Chem 1989:295–311.
Westerhoff P, Chen W, Esparza M. Fluorescence analysis of a standard fulvic acid on tertiary treated wastewater. J Environ Qual 2001;30:2037–46.
Worrall F, Harriman R, Evans CD, Watts CD, Adamson J, Neal C, et al. Trends in dissolved organic carbon in UK rivers and lakes. Biogeochemistry 2004;70:369–402.
Wu F, Tanoue E. Molecular mass distribution and fluorescence characteristics of dissolved organic ligands for copper (II) in Lake Biwa, Japan. Org Geochem 2001;32:11–20.
Zepp RG, Sheldon WM, Moran MA. Dissolved organic fluorophores in southeastern US coastal waters: correction method for eliminating Rayleigh and Raman scattering peaks in excitation–emission matrices. Mar Chem 2004;89:15–36.